# Mindbomb 1, an E3 ubiquitin ligase, forms a complex with RYK to activate Wnt/β-catenin signaling

Jason D. Berndt,[1] Atsushi Aoyagi,[1,2] Peitzu Yang,[1,2] Jamie N. Anastas,[1,2,3] Lan Tang,[1,2] and Randall T. Moon[1,2]

[1]Howard Hughes Medical Institute, Department of Pharmacology, and [2]Institute for Stem Cell and Regenerative Medicine, University of Washington School of Medicine, Seattle, WA 98109
[3]Molecular and Cellular Biology graduate program, University of Washington, Seattle, WA 98109

Receptor-like tyrosine kinase (RYK) functions as a transmembrane receptor for the Wnt family of secreted protein ligands. Although RYK undergoes endocytosis in response to Wnt, the mechanisms that regulate its internalization and concomitant activation of Wnt signaling are unknown. We discovered that RYK both physically and functionally interacts with the E3 ubiquitin ligase Mindbomb 1 (MIB1). Overexpression of MIB1 promotes the ubiquitination of RYK and reduces its steady-state levels at the plasma membrane. Moreover, we show that MIB1 is sufficient to activate Wnt/β-catenin (CTNNB1) signaling and that this activity depends on endogenous RYK. Conversely, in loss-of-function studies, both RYK and MIB1 are required for Wnt-3A–mediated activation of CTNNB1. Finally, we identify the *Caenorhabditis elegans* orthologue of MIB1 and demonstrate a genetic interaction between *ceMIB* and *lin-18/RYK* in vulva development. These findings provide insights into the mechanisms of Wnt/RYK signaling and point to novel targets for the modulation of Wnt signaling.

## Introduction

The Wnt family of secreted glycoproteins plays a critical role in developmental processes including axis patterning, cellular proliferation, planar cell polarity, cell migration, cell fate specification, and neuronal development. In adults, Wnt signaling is involved in tissue homeostasis, regeneration, and stem/progenitor cell function. Moreover, elevated or attenuated Wnt signaling is found in a diversity of diseased tissues (Logan and Nusse, 2004; Moon et al., 2004).

Wnt signaling can be divided into CTNNB1-dependent and CTNNB1-independent signaling. The best-characterized family of receptors for Wnts is the Frizzled class of seven-pass transmembrane atypical G protein–coupled receptors. In addition, CTNNB1-dependent signaling requires a coreceptor, the low-density lipoprotein receptor–related proteins 5 and 6 (LRP). More recently, it has become clear that two additional unrelated, single-pass receptor tyrosine kinases, receptor tyrosine kinase-like orphan receptor 2 (ROR2) and receptor-like tyrosine kinase (RYK), can bind to Wnts. In contrast to signaling events downstream of the Frizzled/LRP receptors, the mechanisms of ROR2- and RYK-mediated Wnt signaling are poorly understood (Angers and Moon, 2009). RYK has been shown to bind to Frizzleds (Lu et al., 2004; Kim et al., 2008; Li et al., 2009). However, Frizzleds are not required for Wnt/RYK signaling in all contexts (Inoue et al., 2004; Schmitt et al., 2006; Harris and Beckendorf, 2007; Li et al., 2009), which suggests a distinct molecular mechanism of Wnt/RYK signaling.

RYK is required for CTNNB1-dependent Wnt signaling, as loss of function of RYK inhibits the ability of Wnt-3A to activate a CTNNB1-dependent transcriptional reporter in human embryonic kidney (HEK293T) cells (Lu et al., 2004). Moreover, RYK is required for Wnt/CTNNB1 signaling in vivo. In the specification of vulva cell fate in *Caenorhabditis elegans*, *LIN-18/RYK* shows a genetic interaction with *WNT/MOM-2* and *TCF/POP-1* (Inoue et al., 2004; Deshpande et al., 2005). In mice, RYK is required for Wnt-3A–induced neurite outgrowth from explanted dorsal root ganglia (Lu et al., 2004)

Correspondence to Randall T. Moon: rtmoon@uw.edu

A. Aoyagi's present address is: Daiichi Sankyo Co., Ltd., Shinagawa-ku, Tokyo 140-8710, Japan.

Abbreviations used in this paper: ICD, intracellular domain; mRYK, mouse Ryk; RYK, receptor-like tyrosine kinase.



The Rockefeller University Press $30.00
J. Cell Biol. Vol. 194 No. 5 737–750
www.jcb.org/cgi/doi/10.1083/jcb.201107021

and neuronal differentiation of neocortical progenitor cells (Lyu et al., 2008).

RYK is also involved in stimulating CTNNB1-independent Wnt signaling pathways. Genetic and biochemical studies demonstrate that Wnt-5 and RYK cooperate to regulate axon pathfinding in vivo and in vitro in multiple species (Liu et al., 2005; Keeble et al., 2006; Wouda et al., 2008; Li et al., 2009; Miyashita et al., 2009). Moreover, Wnt-5 and Wnt-11 signal through RYK to regulate cell movements during convergent extension of zebrafish (*Danio rerio*) and frog (*Xenopus laevis*) embryos (Kim et al., 2008; Lin et al., 2010). Though not directly tested in these studies, Wnt-5 and Wnt-11 have been reported to signal independently of CTNNB1 in a context-dependent manner.

The molecular mechanisms of Wnt/RYK signaling remain elusive. RYK is composed of a leucine-rich extracellular domain with a WIF-type Wnt binding region, a single transmembrane domain, and an intracellular tyrosine kinase domain (Halford and Stacker, 2001). Most evidence suggests that RYK signaling does not depend on intrinsic kinase activity; however, RYK has been shown to interact with other kinases including Ephrin receptors and Src, which suggests cross-talk with other tyrosine kinase signaling cascades (Halford et al., 2000; Trivier and Ganesan, 2002; Kamitori et al., 2005; Wouda et al., 2008). In addition, in neuronal precursor cells, RYK is cleaved by γ-secretase, and treatment with Wnt-3A leads to the nuclear accumulation of the RYK intracellular domain (RYKICD; Lyu et al., 2008). Whether the RYKICD binds to DNA or has any role in the regulation of transcription remains an open question. Finally, two recent studies show that RYK is internalized in response to Wnt-5 and Wnt-11 (Kim et al., 2008; Lin et al., 2010). However, neither the consequences of RYK internalization nor the factors that regulate internalization are known.

In this paper, we identified RYK-associated proteins by affinity purification mass spectrometry and leveraged the results to investigate the mechanisms of Wnt/RYK signaling. Although this approach identified multiple proteins that co-purify with RYK, in this study we focused on the E3 ubiquitin ligase MIB1. Biochemical experiments revealed that MIB1 promotes the ubiquitination and turnover of full-length RYK and results in the loss of RYK expression at the cell surface. Moreover, using both gain- and loss-of-function experiments in vitro and in vivo, we found an as of yet unreported functional relationship between RYK and MIB1 in the positive regulation of Wnt/CTNNB1 signaling.

## Results

### Affinity purification mass spectrometry of RYK

To identify proteins that were candidates for mediating Wnt/RYK signaling, we used tandem affinity purification of RYK followed by mass spectrometry (Angers et al., 2006; Major et al., 2007). We stably expressed glue-tagged RYK at low levels in HEK293T cells, which have intact Wnt/RYK signaling (Lu et al., 2004). We isolated glue-tagged RYK from cells that were treated and lysed under several conditions to identify the maximum number of interaction partners (Table S3). Because RYK is known to be cleaved and internalized, we also performed affinity purification of glue-tagged RYKICD from stably expressing HEK293T cells. Using this combined approach, we identified several known RYK-interacting proteins including CDC37, ubiquitin, HSP90, and ephrin receptors (Fig. 1 A and Table S3; Halford et al., 2000; Trivier and Ganesan, 2002; Kamitori et al., 2005; Lyu et al., 2009). We identified a total of 66 RYK-associated proteins that met the following criteria: (a) the proteins were identified in at least three of eight independent pull-down experiments, (b) the proteins were represented by at least two unique peptides, and (c) the proteins had not been previously identified as common nonspecific contaminants (Gingras et al., 2005; Major et al., 2008).

Using bioinformatic analyses, we classified these proteins into several complexes or families of proteins involved in cell signaling, cell adhesion, cell cycle and apoptosis, actin remodeling, planar cell polarity, ubiquitination, and protein trafficking (Fig. 1 A and Table S4). Among the novel proteins identified, the most frequently observed and the highest in abundance was the E3 ubiquitin ligase MIB1.

### RYK exists in a protein complex with MIB1

To confirm the finding that RYK and MIB1 coexist in a protein complex, we used affinity purification and Western blotting. We found that streptavidin purification of glue-tagged RYK, RYKICD, or of a plasma-membrane tethered, i.e., myristoylated, version of the RYKICD (MYR-RYKICD) efficiently coprecipitated endogenous MIB1 as compared with untransfected HEK293T cells or those expressing glue-tagged negative control proteins (Fig. 1, B and C). Moreover, in the reverse pull-down experiment, flag-tagged MIB1 coprecipitated glue-RYKICD (Fig. 1 D).

Previous studies have shown that substrates of MIB1-mediated ubiquitination bind to its N-terminal MIB/HERC2-type zinc finger (Itoh et al., 2003). Therefore, we performed an analysis to define the domain of MIB1 required for forming a complex with RYK. We transiently expressed a series of flag-tagged N- and C-terminal truncations of MIB1 in cells stably transfected with glue-RYKICD. We found that the RYKICD efficiently coprecipitated with the N terminus of MIB1 (minimal binding domain aa 1–124) but not the C terminus (Fig. 1, B and D). We also observed that RYK could form a complex with a point mutant of MIB1 (C997S) that reduces its enzymatic activity (Fig. 1 D). In summary, these results show that RYK and MIB1 exist in a protein complex in a manner requiring the interaction of the ICD of RYK and the substrate recognition domain of MIB1.

### MIB1 promotes the ubiquitination of RYK

MIB1 acts as an E3 ubiquitin ligase for several substrates (Jin et al., 2002; Itoh et al., 2003; Yoo et al., 2006; Zhang et al., 2007). Thus, we investigated whether MIB1 could promote the ubiquitination of RYK. We performed nickel affinity

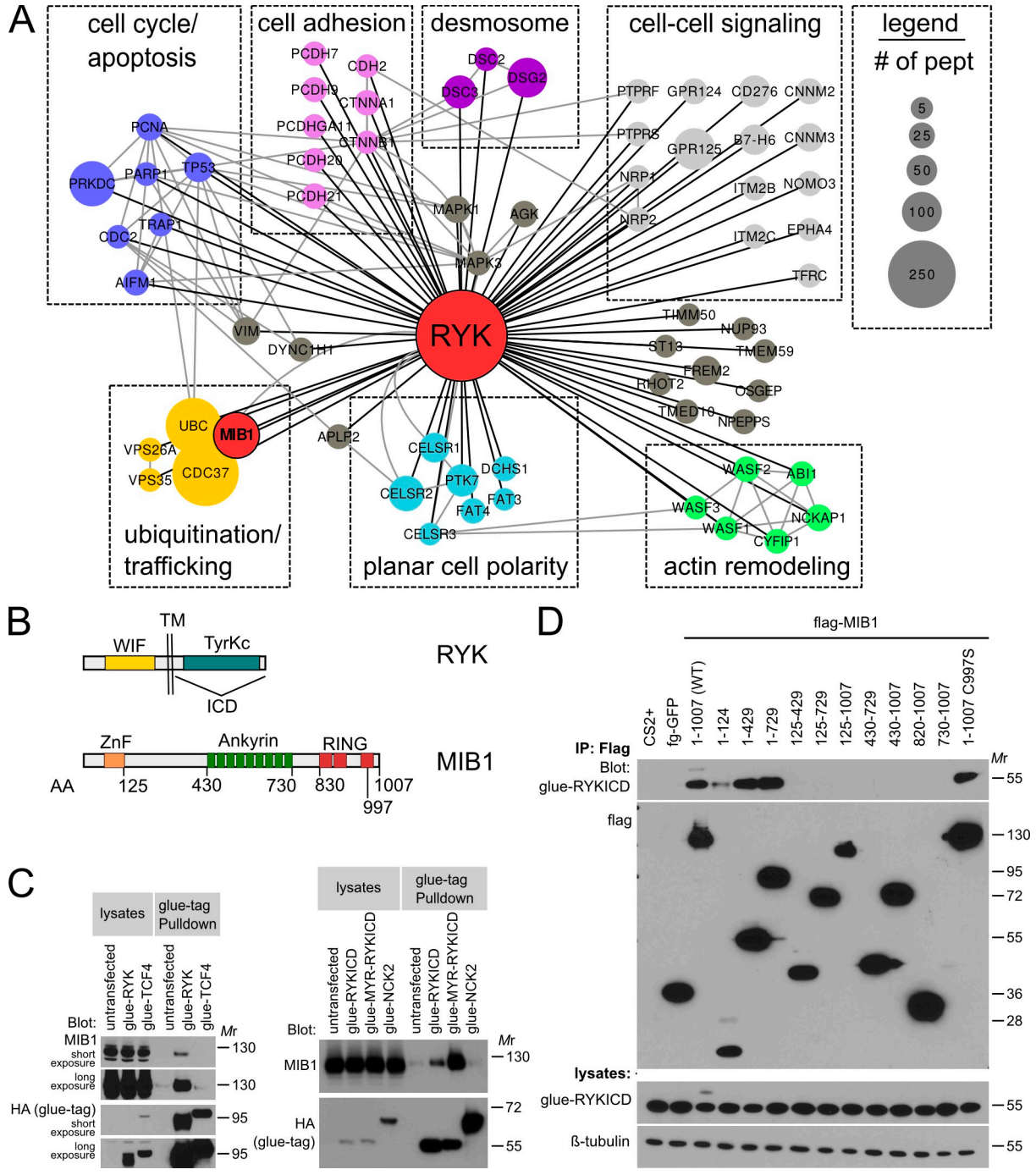


Figure 1. **Affinity purification mass spectrometry identifies MIB1 as a novel interaction partner with RYK.** (A) Illustration depicts the RYK-associated protein interaction network discovered by affinity purification mass spectrometry (black lines). The STRING database was used to curate additional interactions among proteins found to interact with RYK (gray lines). The size of the node indicates the total number of peptides identified in eight independent purifications. (B) Schematic representation of RYK and MIB1 proteins depicting predicted domains. (C) Western blot for endogenous MIB1 demonstrates interaction with streptavidin affinity-purified glue-tagged RYK, RYKICD, or a membrane tethered form of the RYKICD (MYR-RYKICD). Untransfected, glue-TCF4, and glue-NCK2 cells served as negative controls. (D) Western blot for glue-RYKICD demonstrates interactions with flag affinity-purified full-length MIB1, the N terminus of MIB1, or a point mutant (C997S) of MIB1 that renders it catalytically impaired. N-terminally truncated MIB1 and negative controls do not copurify RYK. Blots represent $n > 3$.

purification of urea-denatured HEK293T cell lysates transfected with 6XHIS-ubiquitin, glue-RYK, and flag-MIB1. We found that MIB1 overexpression dramatically increased the level of ubiquitination of RYK (Fig. 2 A). Amino acid substitutions or deletions in the C-terminal enzymatic ring domains of MIB1 have been shown to impair its ability to conjugate ubiquitin to other substrates (Jin et al., 2002; Itoh et al., 2003; Yoo et al., 2006; Zhang et al., 2007). Similarly, we found that MIB1 with a point mutation (C997S) in the third ring domain or MIB1 lacking all three ring domains (aa 1–729; MIB1-ΔRN3) significantly reduced or eliminated, respectively, the ability of MIB1 to promote the ubiquitination of RYK (Fig. 2 A).

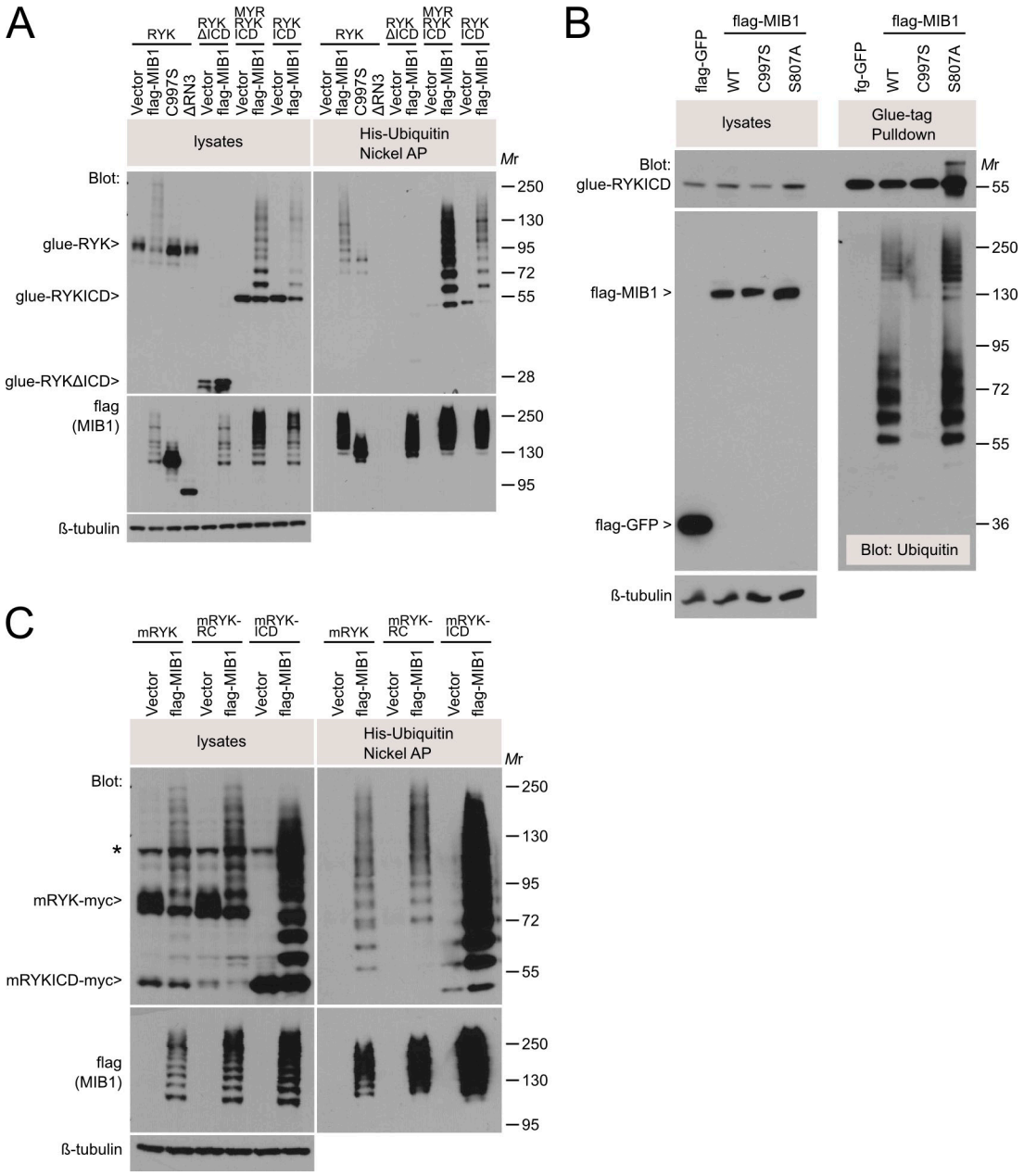


Figure 2. **MIB1 promotes RYK ubiquitination.** (A) Western blot analyzing metal-affinity purification of His-tagged ubiquitin under denaturing conditions. The blot shows that that MIB1 can promote the ubiquitination of the N-terminal glue-tagged RYK, RYKICD, and membrane-tethered MYR-RYKICD but not RYK lacking the ICD (RYKΔICD). Mutant MIB1, C997S, and truncated MIB1, ΔRN3, have little or no catalytic activity with respect to RYK. (B) Western blot analyzing streptavidin purification of glue-RYKICD. The blot shows the conjugation of endogenous ubiquitin promoted by MIB1 and by nonphosphorylatable MIB1-S807A, but not by MIB1-C997S. (C) Western blot analyzing metal affinity purification of His-tagged ubiquitin under denaturing conditions showing that MIB1 can promote the ubiquitination of C-terminal myc-tagged mouse RYK, RYKICD, and noncleavable RYK-RC. Blots represent $n > 3$. The asterisk indicates a nonspecific band.

In addition, we found that MIB1 could efficiently promote the ubiquitination of glue-tagged RYKICD or MYR-RYKICD but not RYKΔICD, which lacks the ICD, (Fig. 2 A); this suggests that MIB1 acts on the cytoplasmic tail of RYK. Therefore, MIB1 is sufficient to promote the covalent addition of ubiquitin to RYK in a manner that depends on the intrinsic enzymatic activity of MIB1.

We next investigated whether MIB1 could enhance the conjugation of endogenous ubiquitin to RYK. Cells transfected with MIB1 but not MIB1-C997S robustly increased the ubiquitin immunoreactivity of streptavidin affinity-purified glue-RYKICD (Fig. 2 B). In addition, a point mutation in MIB1 (S807A) that inhibits phosphorylation by PAR1 and subsequent autoubiquitination (Ossipova et al., 2009) did not interfere with the ubiquitination of RYK (Fig. 2 B). Thus, MIB1 is sufficient to promote the ubiquitination of RYK in the absence of exogenous ubiquitin.

Mouse Ryk (mRYK) shares 93% amino acid identity with human RYK and 98% identity within the ICD, including 18 of 19 lysines. mRYK is cleaved by γ-secretase and the

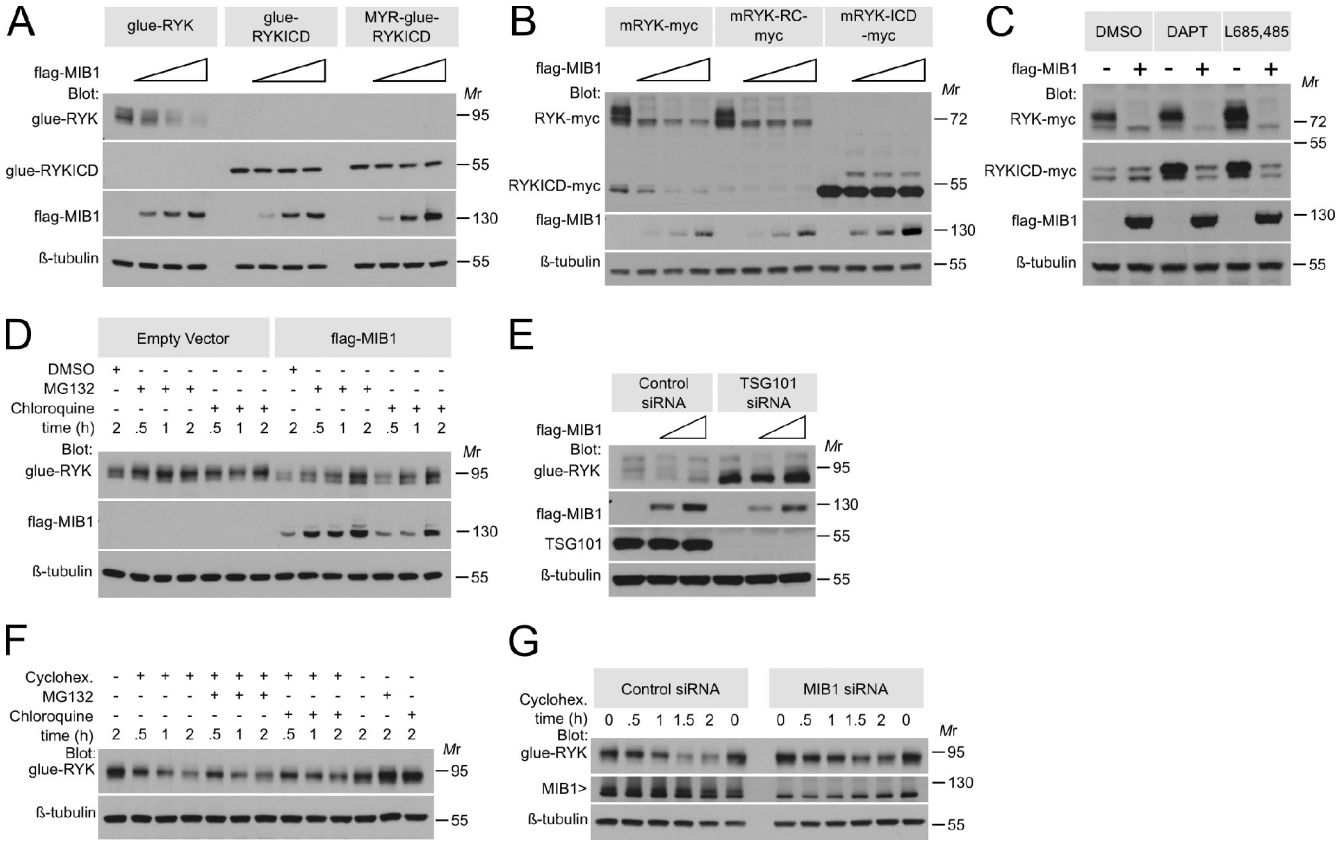


Figure 3. **MIB1 promotes RYK protein turnover.** (A) Western blot of cell lysates showing that MIB1 cDNA overexpression results in a decrease in full-length RYK but not RYKICD or MYR-RYKICD. (B) Western blot of cell lysates showing that MIB1 cDNA overexpression results in a decrease in full-length mouse RYK and noncleavable RYK-RC but not mouse RYKICD. (C) Western blot of cell lysates showing that MIB1 cDNA overexpression results in a decrease in full-length mouse RYK in the presence of γ-secretase inhibitors. (D) Western blot of cell lysates showing that MIB1-dependent degradation of RYK can be reversed by inhibition of the proteasome with MG132 or inhibition of the lysosome with chloroquine. (E) Western blot of cell lysates demonstrating that the inhibition of the expression of TSG101, a member of the ESCRT pathway, reverses the ability of MIB1 to degrade RYK. (F) Western blot of cell lysates demonstrating that the turnover of full-length RYK in the presence of translation inhibition by cycloheximide can be reversed with proteasome or lysosome inhibition. (G) Western blot of cell lysates demonstrating that the turnover of full-length RYK in the presence of cycloheximide can be reversed by knockdown of MIB1 with siRNAs. Blots represent $n = 3$.

ICD cleavage product has been shown to be ubiquitinated and degraded in the proteasome (Lyu et al., 2009). Therefore, we asked whether MIB1 could ubiquitinate mRYK by expressing C-terminally myc-tagged mRYK in combination with 6XHIS-ubiquitin and human flag-MIB1. Similar to our results with human RYK, we found that MIB1 could efficiently ubiquitinate mRYK and mRYKICD. In addition, we found that MIB1 could ubiquitinate mRYK-RC, a form of full-length mRYK that is resistant to γ-secretase cleavage (Fig. 2 C; Lyu et al., 2009). These results demonstrate that MIB1-mediated ubiquitination of RYK is not species-specific nor an artifact of the type or position of the epitope tag. Moreover, ubiquitination by MIB1 does not depend on γ-secretase–mediated cleavage of RYK. In summary, our results with human and mouse RYK indicate that MIB1 is sufficient to promote the ubiquitination of RYK.

### MIB1 promotes the turnover of RYK

We next tested the hypothesis that MIB1 overexpression decreases RYK protein levels. We found that the steady-state levels of full-length glue-RYK were decreased by MIB1 in a dose-dependent manner (Fig. 3 A). In contrast, neither glue-RYKICD nor the plasma membrane–tethred form, MYR-glue-RYKICD, were significantly decreased by overexpression of MIB1 (Fig. 3 A). We also tested whether C-terminal myc-tagged mRYK levels were affected by MIB1. Consistent with our results with human RYK, overexpression of MIB1 decreased the levels of full-length mRYK-myc but not of mRYK-ICD-myc (Fig. 3 B). Thus, MIB1 can promote the turnover of full-length RYK but not the RYKICD. We also discovered that the levels of mRYK-RC-myc were decreased by MIB1 (Fig. 3 B). This result suggested that γ-secretase cleavage is not required for the ability of MIB1 to degrade RYK. Indeed, in a direct test of this hypothesis we found that MIB1 was able to degrade wild-type full-length mRYK-myc in the presence of either of two small molecule inhibitors of γ-secretase activity (Fig. 3 C). Collectively, these data demonstrate that the extracellular region of RYK is required for efficient turnover and imply the presence of additional regulatory factors.

We next tested whether the inhibition of the proteasome or lysosome could restore RYK levels in the presence of overexpressed MIB1. We found that addition of either MG132 or chloroquine, small molecule inhibitors of the proteasome and lysosome, respectively, resulted in increased steady-state levels

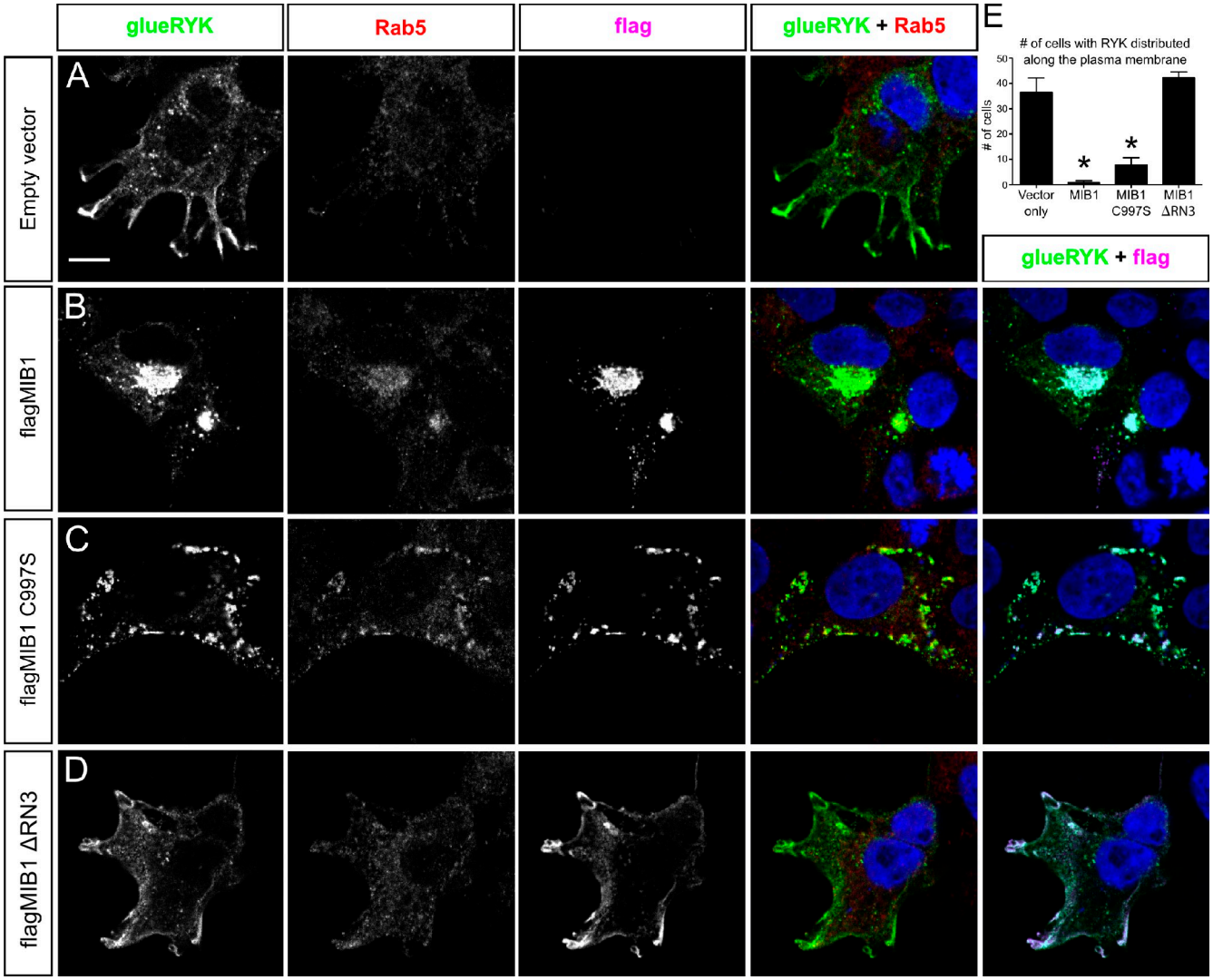


Figure 4. **MIB1 colocalizes with RYK on intracellular membranes.** (A–D) Single-plane confocal images of immunofluorescent labeling of HEK293T cells transiently transfected with cDNA encoding full-length glue-tagged RYK and flag-tagged MIB1 or variants of MIB1. RYK is primarily localized to the plasma membrane when expressed alone (A). However, when overexpressed with MIB1 (B), RYK and MIB1 colocalize to intracellular membranous organelles that are also positive for Rab5. Catalytically impaired MIB1-C997S colocalizes with RYK in aggregates at or near the plasma-membrane (C). In contrast, overexpression of MIB1 lacking all three enzymatic domains MIB1-ΔRN3 (D) minimally affects RYK surface localization and colocalizes at the sites of cell protrusions. (E) Quantification of immunocytochemistry demonstrating that MIB1 and MIB1-C997S reduce the distribution of RYK along the plasma membrane. Data are mean + SEM (error bars). *, $P < 0.005$ (Student's *t* test, $n = 4$). Bar, 10 µm.

of glue-RYK and inhibited the ability of MIB1 to degrade glue-RYK (Fig. 3 D). Trafficking of ubiquitinated cargo to the lysosome depends on members of the ESCRT pathway, such as TSG101 (Raiborg and Stenmark, 2009). Therefore, to further test whether MIB1 overexpression leads to lysosomal degradation of RYK, we assessed levels of glue-RYK in the context of TSG101 inhibition by siRNA. We found that *TSG101* siRNA transfection increased steady-state levels of RYK and inhibited the ability of MIB1 to degrade RYK (Fig. 3 E). Collectively these results show that MIB1 overexpression is sufficient to promote the degradation of RYK by the proteasome and the lysosome.

The findings in Fig. 3 imply that endogenous MIB1 could regulate the rate of RYK turnover. To test whether endogenous MIB1 is required for RYK degradation, we first monitored the expression of full-length glue-RYK after inhibition of protein translation with cycloheximide. We found that RYK levels decreased within 2 h of cycloheximide treatment (Fig. 3 F). Moreover, we found that we could delay the rate of RYK turnover by simultaneously treating cells with proteasome or lysosome inhibitors consistent with ongoing RYK turnover by these organelles (Fig. 3 F).

Next, we transfected cells with control or *MIB1* siRNAs and evaluated RYK turnover. Importantly, we found that the degradation of RYK in cycloheximide-treated cells was delayed by MIB1 loss of function (Fig. 3 G). These results support a model in which endogenous MIB1 promotes the turnover of full-length RYK through ubiquitination and degradation.

### MIB1 colocalizes with RYK on Rab5-positive intracellular membranes

We also investigated the subcellular localization of RYK and MIB1. When glue-RYK was expressed in either HEK293T or Hela cells, it localized to the plasma membrane and intracellular

vesicles (Fig. 4 A and Fig. S2 A). However, when RYK was coexpressed with flag-MIB1, both proteins colocalized on large intracellular membrane and vesicular organelles (Fig. 4, B and E; and Fig. S2 B). Notably, these organelles were also positive for the endocytic marker Rab5 (Fig. 4 B; Sorkin and von Zastrow, 2009).

Because MIB1 ubiquitinates RYK, we also asked whether the enzymatic activity of MIB1 was required for the relocalization of RYK. Co-expression of MIB1-C997S with RYK resulted in colocalization in protein aggregates or aggregated vesicles near the plasma membrane and in intracellular vesicles (Fig. 4, C and E; and Fig. S2 C). As with wild-type MIB1, these structures were also positive for Rab5. Although MIB1-C997S has reduced enzymatic activity, residual ubiquitination of RYK (Fig. 2 A) could account for this change in RYK localization. Thus, we also tested the enzyme-dead MIB1, MIB1-ΔRN3. Unlike MIB1 or MIB1-C997S, MIB1-ΔRN3 had no effect on RYK localization, though both proteins colocalized at sites along the plasma membrane (Fig. 4, D and E; and Fig. S2 D).

### MIB1 quantitatively reduces RYK surface expression in the absence of protein degradation

We next used an independent method to quantify surface RYK expression on individual cells. As we had found that MIB1 regulates RYK protein turnover, MIB1-mediated decreases in total RYK might account for the loss of surface expression of RYK. Moreover, although the images were scored blind, immunocytochemistry is inherently qualitative and subjective. Therefore, we used flow cytometry to quantify the intensity of RYK surface expression in the context of proteasome and lysosome inhibition. HEK293T cells expressing glue-RYK were treated with chloroquine and MG132 for 2 h and then fixed in paraformaldehyde. We then used immunofluorescence under nonpermeabilizing conditions to detect the N-terminal glue epitope of RYK (Fig. 5 A). Using this method, we found that overexpression of MIB1 decreased the surface expression of RYK by >40% as compared with the vector-only control (Fig. 5, B and C). Expression of MIB1-C997S and MIB1-ΔRN3 had little effect on RYK surface expression (Fig. 5, B and C). Moreover, as predicted from the fact that MIB1 does not ubiquitinate RYKΔICD (Fig. 2 A), we found that MIB1 overexpression did not change RYKΔICD surface expression compared with the vector-only control (Fig. 5 D).

We also tested whether endogenous MIB1 regulates surface expression of RYK. As expected, the inhibition of MIB1 expression by siRNA transfection increased surface RYK expression (Fig. 5, E and F). Collectively, these results suggest that MIB1 is both necessary and sufficient for the expression of RYK at the plasma membrane.

### RYK and MIB1 are required for Wnt/CTNNB1 signaling

Because RYK is required for Wnt/CTNNB1 signaling (Lu et al., 2004), we hypothesized that MIB1 might also regulate Wnt signaling. We measured the activity of a luciferase-based transcriptional reporter (CTNNB1-activated reporter or Wnt/β-catenin–activated luciferase reporter [BAR]; Biechele et al., 2009) in HEK293T cells after transfection of siRNAs against RYK or MIB1. Consistent with previously published data (Lu et al., 2004), we found that three independent siRNAs targeting *RYK* (Fig. S1, A and C) inhibited Wnt-3A–dependent activation of BAR by >50% (Fig. 6 A). Importantly, we also found that three independent siRNAs targeting *MIB1* (Fig. S1, B and D) inhibited activation of BAR by Wnt-3A to a similar degree as *RYK* siRNAs (Fig. 6 A).

In addition, we investigated whether *RYK* and *MIB1* loss of function could reduce the expression of endogenous Wnt/CTNNB1 target genes. We found that treating HEK293T cells with Wnt-3A induced a modest increase in the levels of *AXIN2* that could be partially reversed by MIB1 or RYK loss of function (Fig. 6 B). Unpublished results from our laboratory show that the osteosarcoma cell line, U2OS, has a more robust transcriptional response to Wnt-3A than HEK293T cells (unpublished data). Therefore, we also tested whether MIB1 and RYK were required for Wnt/CTNNB1 signaling in U2OS cells. First, we confirmed that siRNAs targeting either *RYK* or *MIB1* were able to reduce Wnt-3A–mediated activation of BAR in U2OS cells (Fig. 6 C). Likewise, we found that Wnt-3A increased levels of *AXIN2* transcript more than fourfold in the context of control siRNAs and that this effect was significantly reduced by siRNAs targeting either *RYK* or *MIB1* (Fig. 6 D). The expression of another Wnt-target gene, *NKD1*, was also reduced by RYK and MIB1 loss of function in U2OS cells (Fig. 6 E). Finally, we confirmed this effect in a third cell line. As with HEK293T and U2OS, HeLa cells also showed reduced responses to expression of the Wnt-3A–induced target genes *AXIN2*, *NKD1*, and *TNFRSF19* after RYK or MIB1 loss of function (Figs. 6 F and S2, E and F). In summary, these results demonstrate that endogenous RYK and MIB1 are required for Wnt/CTNNB1-dependent transcription in multiple cell lines.

### MIB1 and RYK act upstream of CTNNB1 stabilization

Our data suggest that MIB1 regulates RYK by inhibiting its localization at the cell surface. Thus, RYK and MIB1 loss of function could inhibit activation of Wnt/CTNNB1 signaling by affecting other components of the signaling pathway that operate near the plasma membrane. We found that siRNAs targeting either *RYK* or *MIB1* inhibited the activation of BAR in cells overexpressing Wnt-3A or Disheveled 3 but had little effect on BAR activation by CTNNB1 or stabilized mutant CTNNB1 (CTNNB1*; S33A, S37A, T41A, and S45A; Fig. 7 A). Thus, RYK and MIB1 likely regulate events that occur early in Wnt pathway activation.

To further investigate the temporal requirement for MIB1 in Wnt signaling, we performed a time-course analysis of HEK293T cells treated with Wnt-3A. We found that cells transfected with *MIB1* siRNA show reduced levels of phospho-LRP6, an early marker of Wnt activation, within 30 min of Wnt-3A treatment (Fig. 7 B; Davidson et al., 2005; Zeng et al., 2005). MIB1 loss of function inhibited the ability of Wnt-3A to reduce serine/threonine phosphorylation of CTNNB1; however, we did not see robust changes in Wnt-3A–induced steady-state levels of total CTNNB1 with *MIB1* siRNA (Fig. 7 B).

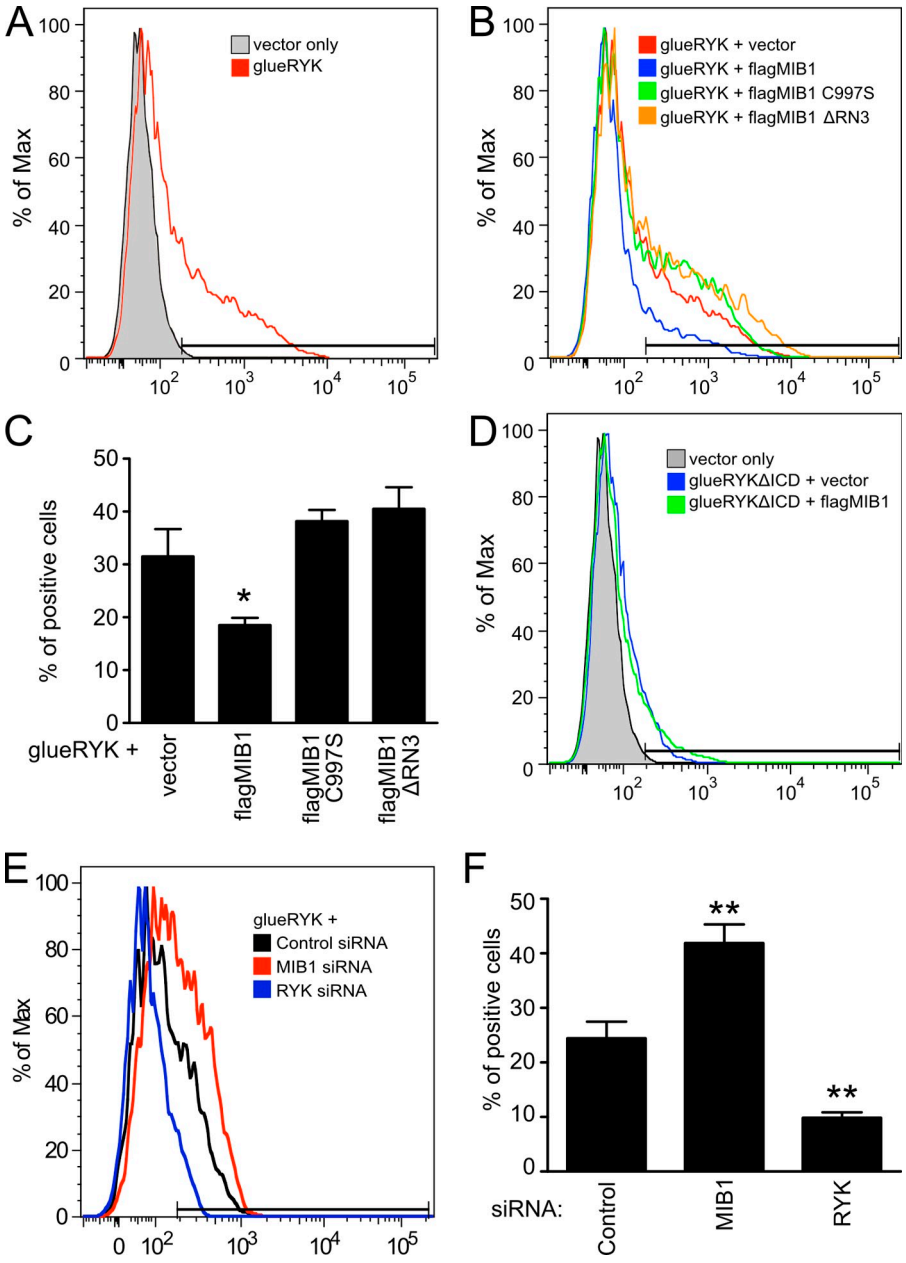


Figure 5. **MIB1 quantitatively reduces RYK surface expression in the absence of protein degradation.** (A, B, D, and E) Histograms of individual cell fluorescence intensities depicting the distribution of surface labeling of RYK in nonpermeabilized HEK293T cells treated for 2 h with chloroquine and MG132, labeled, and then analyzed by flow cytometry. (A) Histogram shows the background of anti-HA immunoreactivity in vector only as compared with glue-RYK–transfected cells. Background intensity was used to determine the RYK-positive gate in each experiment individually. (B) Histogram of surface RYK expression on cells transfected with glue-RYK and vector only or flag-MIB1 or flag-MIB1 mutants. (C) Graph represents the number of cells in the RYK-positive gate shown in B. Data demonstrate a significant decrease in surface RYK expression when cotransfected with MIB1 but not MIB1-C997S or MIB1-ΔRN3. Data are mean + SD (error bars). *, $P < 0.05$. (Student's *t* test, $n = 3$). (D) Histogram of surface RYK expression on cells transfected with N-terminal glue-tagged RYKΔICD and with or without flag-MIB1. (E) Histogram of surface RYK expression on cells transfected with glue-RYK and control, MIB1, or RYK siRNAs. (F) Graph representing the number of cells in the RYK-positive gate shown in E. Data demonstrate that MIB1 loss of function significantly increases the level of RYK expression on the cell surface. Data are mean + SD (error bars). **, $P < 0.005$. (Student's *t* test, $n = 3$).

HEK293T cells have high levels of membrane-associated CTNNB1, and levels of CTNNB1 are not appreciably changed by Wnt-3A treatment. Therefore, we also blotted for CTNNB1 in the lysates that had been stripped of junctional CTNNB1 using conA-sepharose resin (Miller and Moon, 1997). Using this approach, we found that *RYK* and to a lesser degree *MIB1* siRNAs reduced the ability of Wnt-3A to increase the "signaling pool" of CTNNB1 after 1 h of treatment with Wnt-3A (Fig. 7 C). Like our results in HEK293T cells, we found that the transfection of *RYK* or *MIB1* siRNAs reduced the ability of Wnt-3A to increase LRP6 phosphorylation, reduce CTNNB1 phosphorylation, and stabilize CTNNB1 in U2OS cells (Fig. 7 D). Collectively, our data show that RYK and MIB1 are required for Wnt/CTNNB1 signaling through regulation of protein phosphorylation upstream of CTNNB1 stabilization.

### MIB1 activates Wnt/CTNNB1 signaling in an RYK-dependent manner

Collectively, our data suggest that RYK and MIB1 act together in a complex to regulate Wnt/CTNNB1 signaling. To directly test this model, we first asked whether MIB1 overexpression was sufficient to activate Wnt signaling. Indeed, overexpression of MIB1 activated BAR in a dose-dependent manner in the presence or absence of Wnt-3A (Fig. 8 A). Moreover, we found that MIB1 was sufficient to induce *AXIN2* transcription, the phosphorylation of LRP6, and stabilization of CTNNB1 (Figs. 8, B and C). Second, if MIB1 and RYK act in a protein complex, then MIB1 might require interaction with RYK to activate Wnt/CTNNB1 signaling. We found that, unlike full-length MIB1, N-terminally truncated MIB1 mutants, e.g., aa 125–1,007, which do not form a complex with RYK (Fig. 1 C), cannot activate BAR (Fig. 8 D). Moreover, we found that MIB1 mutants, which can form a complex with

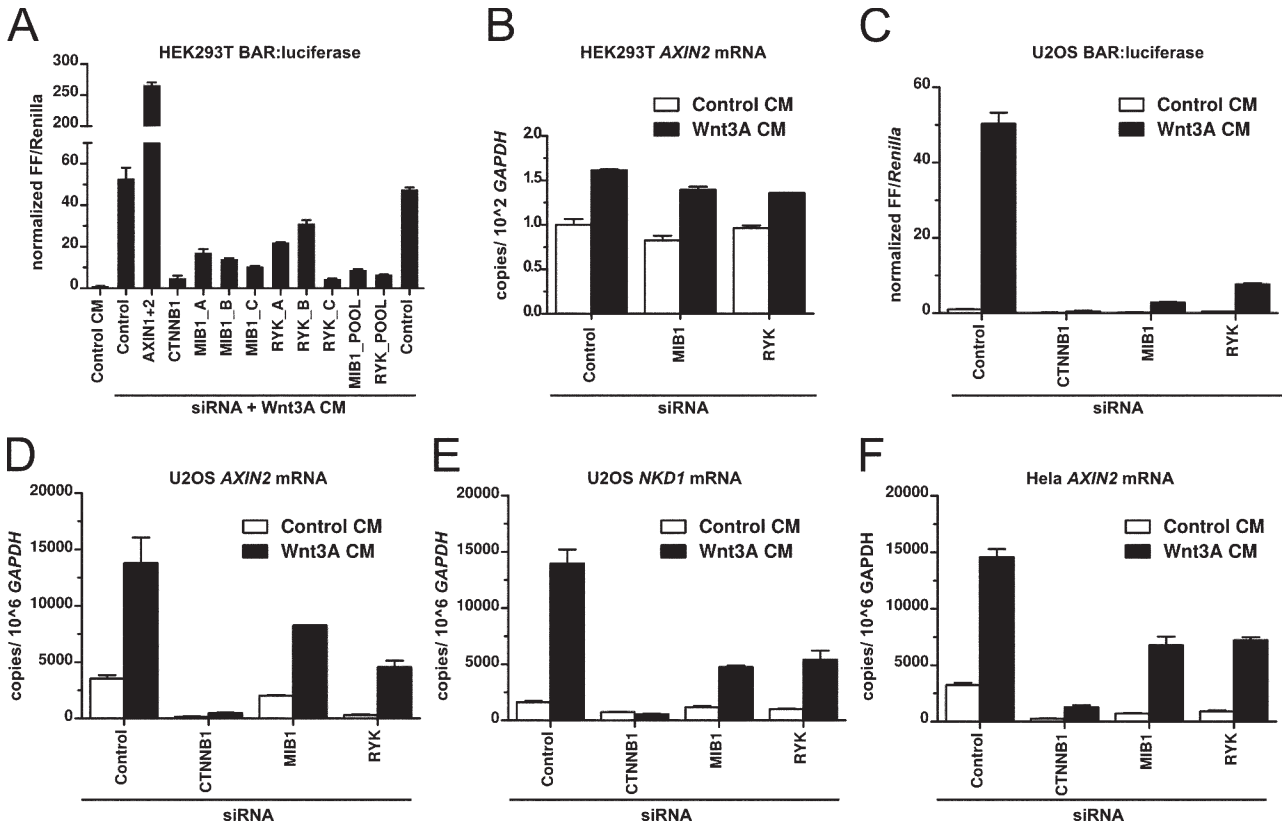


Figure 6. **Endogenous RYK and MIB1 are required for Wnt/CTNNB1 signaling.** (A and C) Graphs showing results from a Wnt/CTNNB1-activated luciferase-based reporter (BAR). Data are mean + SD (error bars). (B and D–F) Quantitative RT-PCR data showing a requirement for RYK and MIB1 in the expression of Wnt target genes in multiple cell lines. Data are mean + SD (error bars). (A) HEK293T cells were transfected with siRNAs for 2 d and then treated overnight with control or Wnt-3A–conditioned media. Results are normalized to one for unstimulated cells. Multiple nonoverlapping siRNAs targeting either *RYK* or *MIB1* significantly reduce Wnt-3A–mediated reporter activation. Data are representative of $n > 5$ experiments. (B) Increases in AXIN2 mRNA levels resulting from treatment with Wnt-3A–conditioned media are reduced in the context of MIB1 or RYK siRNA transfection in HEK293T cells. (C) Graph showing that MIB1 and RYK are required for Wnt-3A–mediated activation of BAR in U2OS cells treated as in A. $n = 5$. (D, E, and F) Graphs showing the results of quantitative RTPCR for *AXIN2* (D and F) and *NKD1* (E), demonstrating a requirement for MIB1 and RYK for the activation of endogenous Wnt-target genes by Wnt-3a in U2OS and HeLa cells. $n = 3$.

RYK but lack enzymatic activity toward RYK, e.g., C997S or ΔRN3 (Figs. 1 C and 2 A), also failed to activate BAR (Fig. 8, A and D). Third and most importantly, if RYK and MIB1 act in the same molecular complex leading to activation of Wnt/CTNNB1 signaling, then the inhibition of RYK expression should reduce the ability of MIB1 overexpression to activate BAR. In fact, we found that *RYK* siRNA transfection significantly inhibited the ability of MIB1 to activate BAR (Fig. 8 E). Thus, MIB1-induced activation of Wnt/CTNNB1 signaling requires the presence and binding of endogenous RYK. Moreover, these data show that MIB1 enzymatic activity is required to activate Wnt signaling. Whether the ubiquitination of RYK by MIB1 is required for Wnt activation remains an open question. However, these data strongly support a model in which endogenous RYK and enzymatically active MIB1 form a complex that has the ability to activate or enhance Wnt/CTNNB1 signaling.

### *C. elegans MIB1* RNAi genetically interacts with *lin-18/RYK*

Wnt signaling is required for vulva cell fate determination in *C. elegans* (Inoue et al., 2004). Mutations of *lin-18/RYK* disrupt the oriented division of p7.p vulval precursor cells, ultimately resulting in a bivulva phenotype. Thus, we asked whether MIB1 was also important in this process. First, we performed BLASTp analysis to identify the *C. elegans* homologue of human MIB1. We identified the protein, Q9U2C5, in the UniProt database. Using reverse BLASTp analysis, we found that Q9U2C5 has equal identity with human MIB1 and MIB2 (23%), which is consistent with the existence of a single ancestral protein (Fig. 9 A). Similar to human MIB1 and MIB2, Q9U2C5 contains seven predicted Ankyrin repeats and two C-terminal ring fingers. The gene encoding Q9U2C5, *Y47D3A.22*, has predicted genetic interactions with several members of the Notch pathway, including *crb-1/Crumbs*, *glp-1/Notch*, *F10D7.5/Neuralized*, and *lin-12/Notch*, which suggests conservation of function with human MIB1 and MIB2 in Delta/Notch signaling (Zhong and Sternberg, 2006). Therefore, we reasoned that Q9U2C5/*Y47D3A.22*, henceforth ceMIB, could be a functional homologue of human MIB1.

We next turned to loss of function in vivo to assess whether *ceMIB* was important for vulva cell fate determination. We found that RNAi targeting *ceMIB* resulted in 24% of worms with the bivulva phenotype (Fig. 9, B and E), which suggests that *ceMIB*, as with *lin-18/RYK*, is important for p7.p orientation. Mutations in *lin-12/Notch* also disrupt vulva development

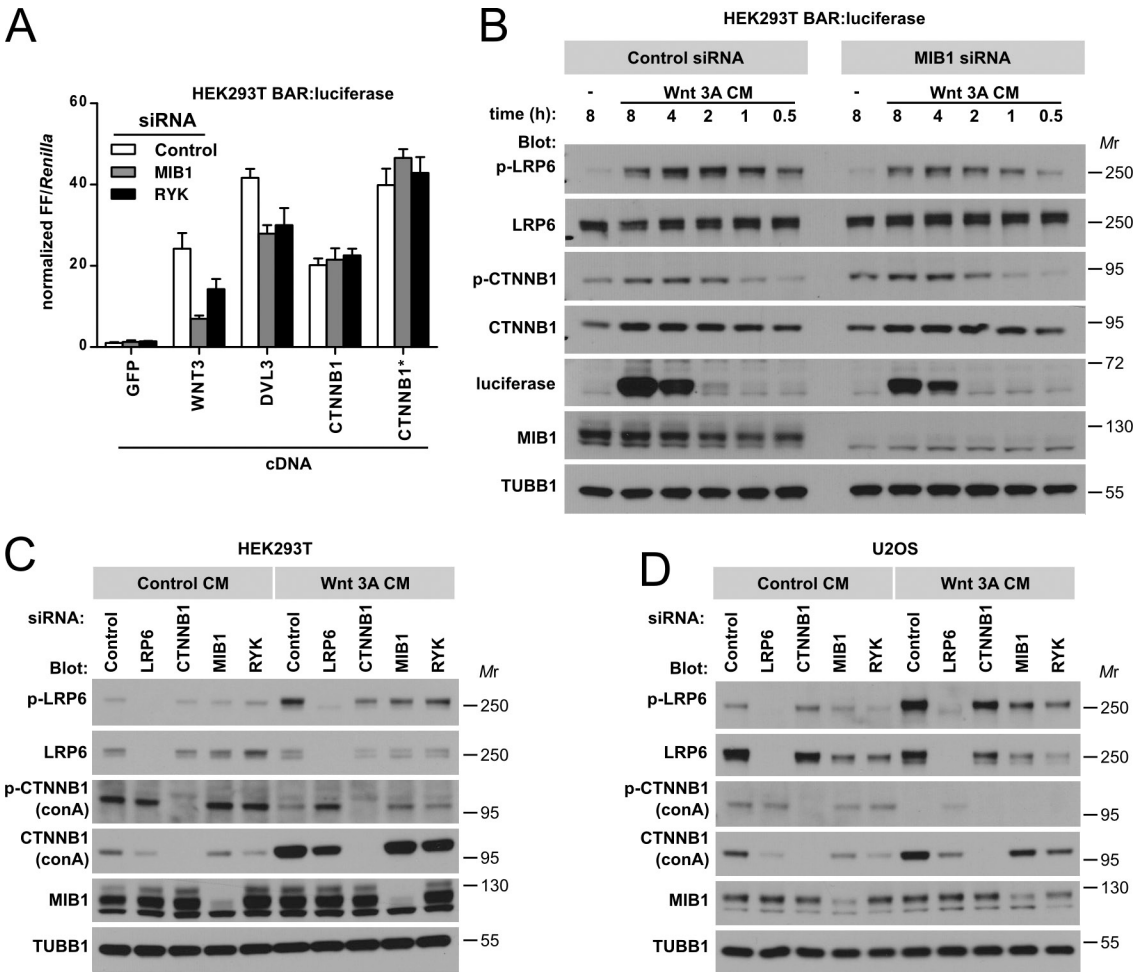


Figure 7. **Endogenous RYK and MIB1 are required for Wnt/CTNNB1 signaling at the level of receptor activation.** (A) RYK and MIB1 siRNA transfection inhibits cDNA overexpression-mediated activation of BAR by Wnt-3A and Disheveled (DVL3) but not CTNNB1 or nondegradable CTNNB1* (S33A, S37A, T41A, and S45A). Data are mean + SD (error bars). (B) Western blot of cell lysates after a time course of treatment with Wnt-3A–conditioned media in cells transfected with control or MIB1 siRNAs. (C) Western blot after 1 h of treatment with Wnt-3A–conditioned media in HEK293T cells transfected with the indicated siRNAs. In rows labeled conA, cell lysates were stripped of membrane-associated proteins by overnight incubation with conA Sepharose resin. (D) Western blot after 1-h treatment with Wnt-3A–conditioned media in U2OS cells transfected with the indicated siRNAs. Blots represent $n = 3$.

(Greenwald et al., 1983). Therefore, we performed experiments to assess the genetic interaction between *ceMIB* and *lin-18/RYK*. Importantly, we found that *ceMIB* RNAi enhanced the penetrance of the bivulva phenotype in the *lin-18/RYK(e620)* mutant (Fig. 9, B and F). Collectively, although these results cannot rule out the possibility that MIB could regulate both Wnt and Notch signaling in vulva development, they do support a role for *ceMIB* in the regulation of *C. elegans* Wnt/RYK/TCF signaling and imply that the role of RYK and MIB1 in Wnt signaling is conserved in vivo and across diverse animal phyla.

## Discussion

Our goal was to investigate novel mechanisms involved in the regulation of Wnt/RYK signaling. We identified MIB1 as a novel protein interaction partner with RYK. We found that overexpressed RYK and MIB1 colocalized and that the overexpression of MIB1 leads to the loss of surface RYK expression. In addition, biochemical studies revealed that MIB1 promotes the ubiquitination and degradation of RYK. We found that MIB1 overexpression activates Wnt/CTNNB1 signaling in an RYK-dependent manner and that endogenous RYK and MIB1 were required for the Wnt-dependent activation of Wnt/CTNNB1 signaling. Finally, we discovered that *lin-18/RYK* and *ceMIB* show a genetic interaction in *C. elegans* vulva development. These findings raise several interesting questions surrounding the relationship of RYK and MIB1 to Wnt signaling.

Does MIB1 regulate RYK trafficking in response to Wnt? Recent studies demonstrate that RYK undergoes endocytosis in response to Wnt binding in vivo (Kim et al., 2008; Lin et al., 2010). We found that MIB1 regulated surface expression of RYK. However, we were unable to detect changes in the surface localization of RYK after treatment with Wnt-3A in our system (unpublished data). Thus, we could not test whether MIB1 was required for Wnt-induced changes in RYK surface expression. Nevertheless, it remains formally possible that MIB1 regulates the endocytosis of RYK after ligand binding.

What is the significance of MIB1-associated RYK ubiquitination? The ubiquitination of transmembrane proteins can lead to endocytosis and trafficking to a variety of intracellular

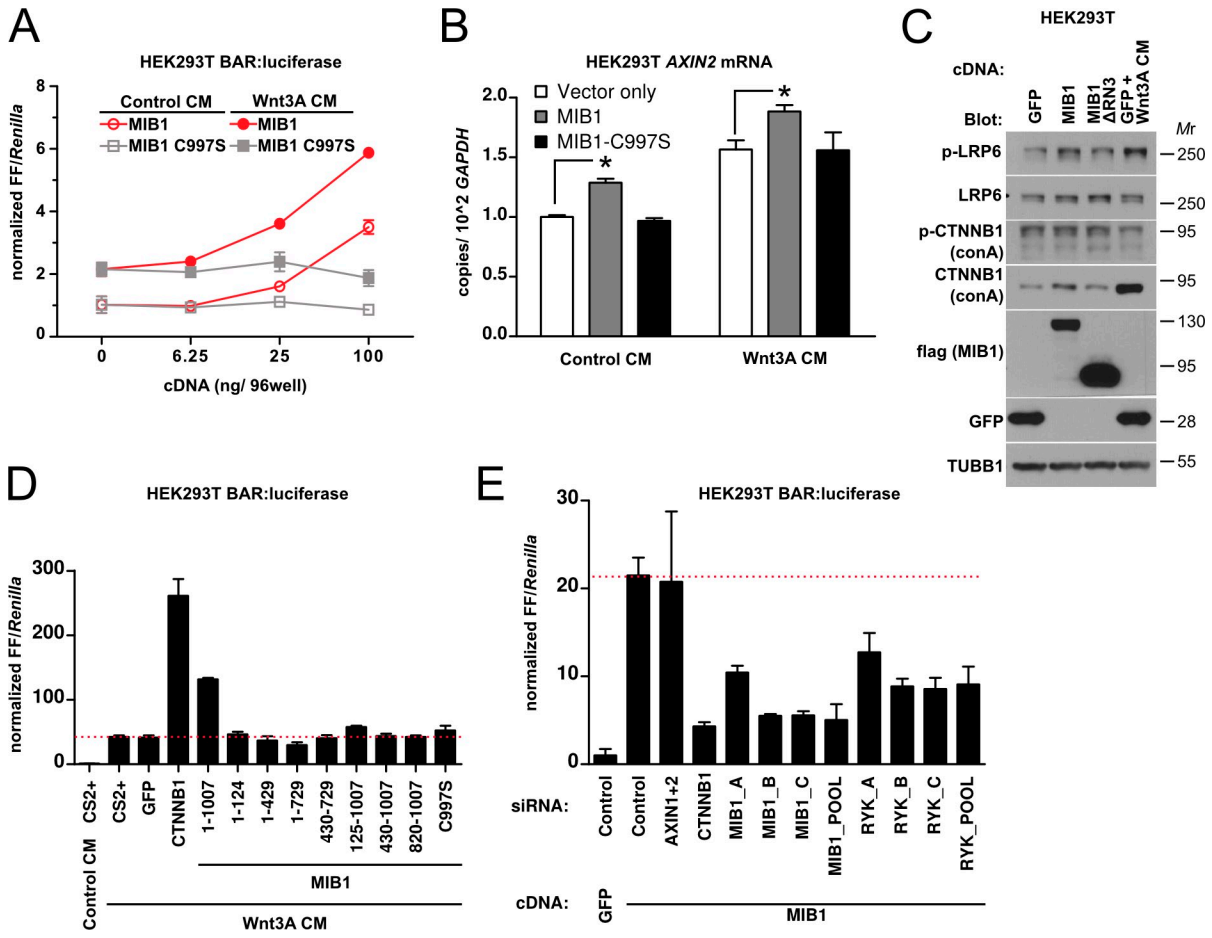


Figure 8. **MIB1 requires endogenous RYK to activate Wnt/CTNNB1 signaling.** (A) Graph demonstrating that MIB1 cDNA overexpression but not catalytically impaired MIB1-C997S can activate BAR in the presence or absence of Wnt-3A–conditioned media. Cells were transfected 6–8 h before treatment with conditioned media overnight. Data are mean + SD. $n = 3$. (B) Data generated from quantitative RT-PCR or HEK293T cells overexpressing MIB1 showing activation of the Wnt target gene, *AXIN2*. Data are mean + SD (error bars). *, $P < 0.05$ using a Student's *t* test. $n = 3$. (C) Western blot of HEK293T cells overexpressing MIB1 showing that MIB1 can activate LRP6 phosphorylation and stimulate CTNNB1 stabilization. In rows labeled conA, cell lysates were stripped of membrane-associated proteins by overnight incubation with conA Sepharose resin. Blot represents $n = 3$. (D) Data showing the enhancement of Wnt-3A–induced BAR activity by the overexpression of MIB1 but not by mutants of MIB1 that lack the ability to bind RYK or lack enzymatic activity. The dotted line indicates the level of reporter activation by Wnt-3A–conditioned media alone. Data are mean + SD (error bars). $n = 3$. (E) Data demonstrating that MIB1-mediated activation of BAR is reversed by multiple independent siRNAs targeting either CTNNB1 or RYK. The dotted line indicates the level of reporter activation by MIB1 overexpression alone. Data are mean + SD (error bar). $n = 3$.

organelles (Sorkin and von Zastrow, 2009). We observed that overexpressed MIB1 promotes the ubiquitination of RYK and loss of surface expression. MIB1 also promotes the ubiquitination and endocytosis of the Notch ligand, Delta (Itoh et al., 2003). Ubiquitination of Delta by MIB1 is thought to promote trafficking through the recycling endosome and further maturation by post-translational modification (Itoh et al., 2003; Hamel et al., 2010). Our biochemical data suggest that MIB1 promotes RYK degradation by the lysosome. However, our experiments do not rule out the possibility that physiological levels of MIB1 alter the subcellular trafficking of RYK in the absence of RYK degradation.

How does MIB1 activate Wnt/CTNNB1 signaling? RYK is required for Wnt/CTNNB1 signaling both in vitro and in vivo (Lu et al., 2004; Inoue et al., 2004; Deshpande et al., 2005; Lyu et al., 2008; this paper). Likewise, we found that MIB1 loss of function inhibits Wnt/CTNNB1 signaling. Paradoxically, we also showed that MIB1 overexpression activates Wnt signaling yet degrades RYK. One possible explanation is that MIB1 ubiquitination of RYK signals the endocytosis of a multimeric complex composed of RYK and other Wnt receptors. The endocytosis of LRP6 and Frizzled has been shown to be required for efficient activation of Wnt/CTNNB1 signaling (Yamamoto et al., 2006; Yamamoto et al., 2008). Consistent with this model, we found that the knockdown of RYK or MIB1 leads to reduced LRP6 phosphorylation and levels in response to Wnt. Whether MIB1 directly regulates the kinases necessary for LRP6 phosphorylation is unknown.

A second possibility is that MIB1 acts downstream of RYK. In this model, the ubiquitination/degradation of RYK could reflect a negative feedback loop regulating RYK surface expression. The kinase MARK (microtubule affinity regulating kinase)/PAR1 can phosphorylate and modulate the function of MIB1 (Ossipova et al., 2009). PAR1 is also known to bind the membrane-associated Wnt pathway protein Disheveled (Sun et al., 2001). Thus, Wnt signaling through RYK could modulate PAR1 phosphorylation of MIB1 and its subsequent activity on

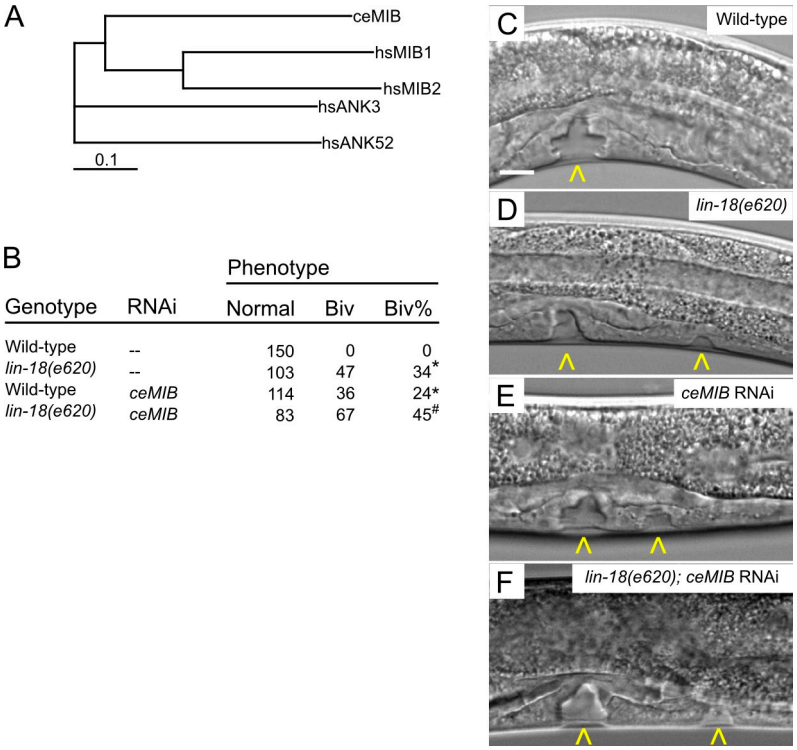


Figure 9. ***C. elegans MIB1* RNAi genetically interacts with *lin-18/RYK*.** (A) Phylogram representing the relationship of ceMIB to the top four hits from a BLASTp analysis of the human proteome. (B) Quantification of the bivulva phenotype from three independent RNAi feeding experiments. *, $P < 0.0001$; #, $P < 0.05$, Fisher's exact test. (C–F) Images of L4 stage *C. elegans* larvae. *ceMIB* RNAi, mutation in *lin-18/RYK*, or the combination of both results in the bivulva phenotype characteristic of abnormal vulva cell fate specification. Anterior is to the left and dorsal is up. Arrowheads indicate vulval invaginations. Bar, 10 µm.

an unknown effector of Wnt signaling. Further studies are needed to assess the biochemical relationships of MIB1, RYK, and other members of the Wnt pathway, and the requirement of MIB1 and RYK for Wnt-mediated changes in protein complexes, posttranslational modification, and localization should help clarify these issues.

In conclusion, we demonstrated the first evidence that the ubiquitin ligase MIB1 acts to regulate Wnt/CTNNB1 signaling in a complex with the Wnt receptor RYK. MIB1 is an important regulator of multiple developmental phenomena, many of which are known to require Wnt signaling. Moreover, because MIB1 acts in other signal transduction pathways, such as Delta/Notch, it represents a novel node for mitigating pathway cross-talk. In the future, it will be important evaluate developmental and disease phenotypes resulting from MIB1 mutation or deletion in the context of both Notch and Wnt signaling.

## Materials and methods

### Cell culture, transfections, and drugs

Hela, HEK293T, and U2OS cells were obtained from the American Type Culture Collection and cultured in DME plus 10% FBS and 1% penicillin/streptomycin (Invitrogen). siRNA transfections were performed with Lipofectamine RNAiMAX (Invitrogen). siRNAs were used singly or in equimolar pools at 20 nM total concentration. siRNA sequences are given in Table S1. cDNA transfections were performed with Lipofectamine 2000 (HEK293T; Invitrogen) or Fugene HD (HeLa; Roche). For protein turnover studies, cells were treated overnight with 10 µM DAPT or 1 µM L-685,485 (both from Tocris Bioscience) or for the indicated times with 10 µg/ml cycloheximide (Sigma-Aldrich), 100 µM chloroquine (Sigma-Aldrich), or 10 µM MG132 (EMD).

### *C. elegans* maintenance and RNAi

Wild-type(N2) and *lin-18(e620)* strains were gifts from the Priess laboratory (Fred Hutchinson Cancer Research Center, Seattle, WA). To identify the *C. elegans* homologue of MIB1, we performed BLASTp analyses using the tools at the National Center for Biotechnology Information and UniProt databases. Phylogenetic analysis was performed with ClustalW2 using the neighbor joining method. Full-length *Y47D3A.22/ceMIB* was amplified from a pool of cDNA from mixed stage wild-type (N2) worms and cloned into the L4440 vector for RNAi feeding. To minimize the maternal contribution, worms were fed on RNAi plates for more than two generations before scoring. Live L4 stage larvae were mounted in PBS on glass slides. Differential interference contrast images were collected at room temperature using NIS Elements software and a Plan Fluor 40×/0.90 NA objective lens on an inverted wide-field microscope (TiE; Nikon). Scores represent the sum of three individual experiments.

### Molecular cloning

*RYK* was amplified by PCR (GenBank/EMBL/DDBJ accession no. NM_001005861, base pairs 229–1923) from human fetal cDNA and cloned into a modified pGLUE vector (Angers et al., 2006) using Asc1 and Not1. The signal sequence from *CHRNA7* was added 5′ to the streptavidin-binding peptide in the glue tag (5′-ATGCGGTGCAGCCCCGGCGGCGTGTGGCTGGGCCTGGCCGCCTCTCTGCTTCATGTGAGCCTG-3′). RYK lacking the ICD (base pairs 229–882) was amplified by PCR and cloned into signal sequence pGLUE using AscI and NotI. The ICD of *RYK* was amplified by PCR (base pairs 883–1923) and cloned into pGLUE using AscI and NotI. MYR-GLUE-RYKICD was made by appending the myristoylation sequence of *SRC* (5′-ATGGGTAGCAACAAGAGCAAGCCCAAGGAT-3′) 5′ to the streptavidin-binding peptide in pGLUE-RYKICD. mRYK clones were received from W. Lu (University of Southern California, Los Angeles, CA). All other cDNA clones were generated by standard PCR-based cloning. Whole-plasmid PCR was used for site-directed mutagenesis of *MIB1*. All clones were verified by complete sequencing of the open reading frames.

### Quantitative RT-PCR

RNA was extracted using the RNAeasy RNA extraction kit as per the manufacturer's recommendations (QIAGEN). First-strand cDNA was synthesized using oligodeoxythymidine and random hexamer primers with the Revert-aid kit (Fermentas). Quantitative RT-PCR was performed on a LightCycler 480 using 10 µl reactions (Roche). Primers used are listed in Table S2.

### Immunocytochemistry, immunoprecipitation, and Western blotting

For immunocytochemistry, cells were seeded onto poly-D-lysine (Sigma-Aldrich)-coated coverslips and fixed in 4% paraformaldehyde in PBS at 22°C for 10 min. For overexpression studies, cells were transfected with 100 ng/cm$^2$ of plasmid 18–20 h before fixation. Secondary antibodies

were donkey or goat anti–rat, anti–mouse, or anti–rabbit Alexa Fluor 488, 568, or 647 conjugates (Invitrogen). Cells were counter-stained with DAPI and mounted in ProLong Gold (Invitrogen). Images were collected at room temperature with NIS Elements software on a microscope (Eclipse Ti; Nikon) coupled to a Nikon A1R confocal operating in Galvano mode and using a Plan-Apochromat 60×/1.40 NA oil objective lens (Nikon). Quantification was performed by an observer that was blinded to the treatments. Images were processed for publication using GIMP 2.6.8 and Inkscape 0.47.

For immunoprecipitation and Western blotting, cells were lysed in 50 mM Tris, pH 8.0, 1% Triton X-100, 0.1% SDS, 0.2% sodium deoxycholate, 150 mM sodium chloride, and 2 mM EDTA plus complete protease and phosphatase inhibitors (Roche). Affinity purification was performed for 2–4 h at 4°C with streptavidin-Sepharose (GE Healthcare) or anti-flag M2 affinity gel (Sigma-Aldrich). For metal affinity purification cells, were lysed in 6 M urea, 300 mM sodium chloride, and 10 mM imidazole in 100 mM sodium phosphate buffer, pH 7.4, and purified 2–4 h at 22°C with Ni-NTA agarose (QIAGEN). The His-tagged ubiquitin plasmid was a gift from D. Bohmann (University of Rochester, Rochester, NY).

Primary antibodies used were CTNNB1 (9561 and 9562; Cell Signaling Technology), β-tubulin (T7816; Sigma-Aldrich), flag (F3165 and F7425; Sigma-Aldrich), HA (3F10, 1867423; Roche), LRP6 (2568 and 3395; Cell Signaling Technology), MIB1 (M5948; Sigma-Aldrich), Rab5 (SC-28570; Santa Cruz Biotechnology, Inc.), TSG101 (Ab83; Abcam), and ubiquitin (P4D1, SC-8017; Santa Cruz Biotechnology, Inc.).

### Surface labeling and flow cytometric analysis

Cells were treated for 2 h with 100 µM chloroquine and 10 µM MG132, harvested by trituration, and fixed for 10 min in 1% paraformaldehyde in PBS. N-terminal glue-tagged proteins were detected with an HA antibody for 2 h at room temperature followed by donkey anti–rat Alexa Fluor 488 for 30 min under nonpermeabilization conditions. At least 10,000 events per sample were collected on a FACS Canto II flow cytometer (BD) and analyzed with FlowJo (Tree Star).

### Affinity purification mass spectrometry and bioinformatics

Tandem affinity purification was performed essentially as described previously (Angers et al., 2006; Major et al., 2007; Major et al., 2008). In brief, cell lysates from 15 × 15 cm plates of HEK293T cells were subjected to affinity purification with streptavidin-Sepharose (GE Healthcare). Bound protein complexes were eluted with 50 mM biotin and further purified with calmodulin Sepharose 4B (GE Healthcare). After elution with EGTA, proteins were reduced and alkylated and then trypsinized overnight at 37°C (Promega). Tryptic peptides were separated by reverse phase nano-HPLC (Eksigent) and eluted directly into a LTQ-XL mass spectrometer (ThermoFisher Scientific). Resultant spectra were searched using Sequest and the Transproteomic Pipeline on a Sorcerer2 (Sage N Research). Unfiltered protein datasets are provided in Table S3. After compiling and filtering the data, proteins were submitted to the Search Tool for the Retrieval of Interacting Genes/Proteins (STRING) database to curate known interactions (von Mering et al., 2003). The protein list was also queried on the Database for Annotation, Visualization and Integrated Discovery (DAVID) functional annotation clustering platform to identify protein complex functions (Dennis et al., 2003). Protein interaction networks were created with Cytoscape 2.7.0 (Shannon et al., 2003).

### Online supplemental material

Fig. S1 shows that *RYK* and *MIB1* siRNAs efficiently knock down mRNA and protein. Fig. S2 shows that MIB1 inhibits surface localization of RYK and is required for Wnt/CTNNB1 signaling in Hela cells. Table S1 shows siRNA. Table S2 shows quantitative RT-PCR primer sequences. Table S3 shows proteomics data and conditions. Table S4 shows DAVID functional annotation of proteomics hits. Online supplemental material is available at http://www.jcb.org/cgi/content/full/jcb.201107021/DC1.

We would like to thank T. Biechele, J. Boyd, W. Conrad, P. von Haller, M. B. Major, M. MacCoss, R. Seifert, and A. Zhou for technical assistance and advice.

J.D. Berndt is an associate and R.T. Moon is an investigator of the Howard Hughes Medical Institute. Salary for P. Yang was funded by the Rubicon grant from Netherlands Organization for Scientific Research (NWO; 825.08.020). We thank the Lynn and Mike Garvey Cell Imaging Laboratory for providing instrumentation and support for imaging.

Submitted: 4 July 2011
Accepted: 2 August 2011

## References

Angers, S., and R.T. Moon. 2009. Proximal events in Wnt signal transduction. *Nat. Rev. Mol. Cell Biol.* 10:468–477.

Angers, S., C.J. Thorpe, T.L. Biechele, S.J. Goldenberg, N. Zheng, M.J. MacCoss, and R.T. Moon. 2006. The KLHL12-Cullin-3 ubiquitin ligase negatively regulates the Wnt-beta-catenin pathway by targeting Dishevelled for degradation. *Nat. Cell Biol.* 8:348–357. doi:10.1038/ncb1381

Biechele, T.L., A.M. Adams, and R.T. Moon. 2009. Transcription-based reporters of WNT/beta-catenin signaling. *Cold Spring Harb. Protoc.* 2009:pdb.prot5223. doi:10.1101/pdb.prot5223

Davidson, G., W. Wu, J. Shen, J. Bilic, U. Fenger, P. Stannek, A. Glinka, and C. Niehrs. 2005. Casein kinase 1 gamma couples Wnt receptor activation to cytoplasmic signal transduction. *Nature*. 438:867–872. doi:10.1038/nature04170

Dennis, G. Jr., B.T. Sherman, D.A. Hosack, J. Yang, W. Gao, H.C. Lane, and R.A. Lempicki. 2003. DAVID: Database for Annotation, Visualization, and Integrated Discovery. *Genome Biol.* 4:P3. doi:10.1186/gb-2003-4-5-p3

Deshpande, R., T. Inoue, J.R. Priess, and R.J. Hill. 2005. lin-17/Frizzled and lin-18 regulate POP-1/TCF-1 localization and cell type specification during *C. elegans* vulval development. *Dev. Biol.* 278:118–129. doi:10.1016/j.ydbio.2004.10.020

Gingras, A.-C., R. Aebersold, and B. Raught. 2005. Advances in protein complex analysis using mass spectrometry. *J. Physiol.* 563:11–21. doi:10.1113/jphysiol.2004.080440

Greenwald, I.S., P.W. Sternberg, and H.R. Horvitz. 1983. The lin-12 locus specifies cell fates in *Caenorhabditis elegans*. *Cell*. 34:435–444. doi:10.1016/0092-8674(83)90377-X

Halford, M.M., and S.A. Stacker. 2001. Revelations of the RYK receptor. *Bioessays*. 23:34–45. doi:10.1002/1521-1878(200101)23:1<34::AID-BIES1005>3.3.CO;2-4

Halford, M.M., J. Armes, M. Buchert, V. Meskenaite, D. Grail, M.L. Hibbs, A.F. Wilks, P.G. Farlie, D.F. Newgreen, C.M. Hovens, and S.A. Stacker. 2000. Ryk-deficient mice exhibit craniofacial defects associated with perturbed Eph receptor crosstalk. *Nat. Genet.* 25:414–418. doi:10.1038/78099

Hamel, S., J. Fantini, and F. Schweisguth. 2010. Notch ligand activity is modulated by glycosphingolipid membrane composition in *Drosophila melanogaster*. *J. Cell Biol.* 188:581–594. doi:10.1083/jcb.200907116

Harris, K.E., and S.K. Beckendorf. 2007. Different Wnt signals act through the Frizzled and RYK receptors during *Drosophila* salivary gland migration. *Development*. 134:2017–2025. doi:10.1242/dev.001164

Inoue, T., H.S. Oz, D. Wiland, S. Gharib, R. Deshpande, R.J. Hill, W.S. Katz, and P.W. Sternberg. 2004. *C. elegans* LIN-18 is a Ryk ortholog and functions in parallel to LIN-17/Frizzled in Wnt signaling. *Cell*. 118:795–806. doi:10.1016/j.cell.2004.09.001

Itoh, M., C.-H. Kim, G. Palardy, T. Oda, Y.-J. Jiang, D. Maust, S.-Y. Yeo, K. Lorick, G.J. Wright, L. Ariza-McNaughton, et al. 2003. Mind bomb is a ubiquitin ligase that is essential for efficient activation of Notch signaling by Delta. *Dev. Cell*. 4:67–82. doi:10.1016/S1534-5807(02)00409-4

Jin, Y., E.K. Blue, S. Dixon, Z. Shao, and P.J. Gallagher. 2002. A death-associated protein kinase (DAPK)-interacting protein, DIP-1, is an E3 ubiquitin ligase that promotes tumor necrosis factor-induced apoptosis and regulates the cellular levels of DAPK. *J. Biol. Chem.* 277:46980–46986. doi:10.1074/jbc.M208585200

Kamitori, K., M. Tanaka, T. Okuno-Hirasawa, and S. Kohsaka. 2005. Receptor related to tyrosine kinase RYK regulates cell migration during cortical development. *Biochem. Biophys. Res. Commun.* 330:446–453. doi:10.1016/j.bbrc.2005.02.177

Keeble, T.R., M.M. Halford, C. Seaman, N. Kee, M. Macheda, R.B. Anderson, S.A. Stacker, and H.M. Cooper. 2006. The Wnt receptor Ryk is required for Wnt5a-mediated axon guidance on the contralateral side of the corpus callosum. *J. Neurosci.* 26:5840–5848. doi:10.1523/JNEUROSCI.1175-06.2006

Kim, G.-H., J.-H. Her, and J.-K. Han. 2008. Ryk cooperates with Frizzled 7 to promote Wnt11-mediated endocytosis and is essential for *Xenopus laevis* convergent extension movements. *J. Cell Biol.* 182:1073–1082. doi:10.1083/jcb.200710188

Li, L., B.I. Hutchins, and K. Kalil. 2009. Wnt5a induces simultaneous cortical axon outgrowth and repulsive axon guidance through distinct signaling mechanisms. *J. Neurosci.* 29:5873–5883. doi:10.1523/JNEUROSCI.0183-09.2009

Lin, S., L.M. Baye, T.A. Westfall, and D.C. Slusarski. 2010. Wnt5b-Ryk pathway provides directional signals to regulate gastrulation movement. *J. Cell Biol.* 190:263–278. doi:10.1083/jcb.200912128

Liu, Y., J. Shi, C.-C. Lu, Z.-B. Wang, A.I. Lyuksyutova, X.-J. Song, and Y. Zou. 2005. Ryk-mediated Wnt repulsion regulates posterior-directed growth

of corticospinal tract. *Nat. Neurosci.* 8:1151–1159. (published erratum appears in *Nat. Neurosci.* 2006. 9:147) doi:10.1038/nn1520

Logan, C.Y., and R. Nusse. 2004. The Wnt signaling pathway in development and disease. *Annu. Rev. Cell Dev. Biol.* 20:781–810. doi:10.1146/annurev.cellbio.20.010403.113126

Lu, W., V. Yamamoto, B. Ortega, and D. Baltimore. 2004. Mammalian Ryk is a Wnt coreceptor required for stimulation of neurite outgrowth. *Cell*. 119:97–108. doi:10.1016/j.cell.2004.09.019

Lyu, J., V. Yamamoto, and W. Lu. 2008. Cleavage of the Wnt receptor Ryk regulates neuronal differentiation during cortical neurogenesis. *Dev. Cell*. 15:773–780. doi:10.1016/j.devcel.2008.10.004

Lyu, J., R.L. Wesselschmidt, and W. Lu. 2009. Cdc37 regulates Ryk signaling by stabilizing the cleaved Ryk intracellular domain. *J. Biol. Chem.* 284:12940–12948. doi:10.1074/jbc.M900207200

Major, M.B., N.D. Camp, J.D. Berndt, X. Yi, S.J. Goldenberg, C. Hubbert, T.L. Biechele, A.-C. Gingras, N. Zheng, M.J. Maccoss, et al. 2007. Wilms tumor suppressor WTX negatively regulates WNT/beta-catenin signaling. *Science*. 316:1043–1046. doi:10.1126/science/1141515

Major, M.B., B.S. Roberts, J.D. Berndt, S. Marine, J. Anastas, N. Chung, M. Ferrer, X. Yi, C.L. Stoick-Cooper, P.D. von Haller, et al. 2008. New regulators of Wnt/beta-catenin signaling revealed by integrative molecular screening. *Sci. Signal.* 1:ra12. doi:10.1126/scisignal.2000037

Miller, J.R., and R.T. Moon. 1997. Analysis of the signaling activities of localization mutants of β-catenin during axis specification in *Xenopus*. *J. Cell Biol.* 139:229–243. doi:10.1083/jcb.139.1.229

Miyashita, T., M. Koda, K. Kitajo, M. Yamazaki, K. Takahashi, A. Kikuchi, and T. Yamashita. 2009. Wnt-Ryk signaling mediates axon growth inhibition and limits functional recovery after spinal cord injury. *J. Neurotrauma*. 26:955–964. doi:10.1089/neu.2008.0776

Moon, R.T., A.D. Kohn, G.V. De Ferrari, and A. Kaykas. 2004. WNT and beta-catenin signalling: diseases and therapies. *Nat. Rev. Genet.* 5:691–701. doi:10.1038/nrg1427

Ossipova, O., J. Ezan, and S.Y. Sokol. 2009. PAR-1 phosphorylates Mind bomb to promote vertebrate neurogenesis. *Dev. Cell*. 17:222–233. doi:10.1016/j.devcel.2009.06.010

Raiborg, C., and H. Stenmark. 2009. The ESCRT machinery in endosomal sorting of ubiquitylated membrane proteins. *Nature*. 458:445–452. doi:10.1038/nature07961

Schmitt, A.M., J. Shi, A.M. Wolf, C.-C. Lu, L.A. King, and Y. Zou. 2006. Wnt-Ryk signalling mediates medial-lateral retinotectal topographic mapping. *Nature*. 439:31–37.

Shannon, P., A. Markiel, O. Ozier, N.S. Baliga, J.T. Wang, D. Ramage, N. Amin, B. Schwikowski, and T. Ideker. 2003. Cytoscape: a software environment for integrated models of biomolecular interaction networks. *Genome Res.* 13:2498–2504. doi:10.1101/gr.1239303

Sorkin, A., and M. von Zastrow. 2009. Endocytosis and signalling: intertwining molecular networks. *Nat. Rev. Mol. Cell Biol.* 10:609–622. doi:10.1038/nrm2748

Sun, T.Q., B. Lu, J.J. Feng, C. Reinhard, Y.N. Jan, W.J. Fantl, and L.T. Williams. 2001. PAR-1 is a Dishevelled-associated kinase and a positive regulator of Wnt signalling. *Nat. Cell Biol.* 3:628–636. doi:10.1038/35083016

Trivier, E., and T.S. Ganesan. 2002. RYK, a catalytically inactive receptor tyrosine kinase, associates with EphB2 and EphB3 but does not interact with AF-6. *J. Biol. Chem.* 277:23037–23043. doi:10.1074/jbc.M202486200

von Mering, C., M. Huynen, D. Jaeggi, S. Schmidt, P. Bork, and B. Snel. 2003. STRING: a database of predicted functional associations between proteins. *Nucleic Acids Res.* 31:258–261. doi:10.1093/nar/gkg034

Wouda, R.R., M.R.K.S. Bansraj, A.W.M. de Jong, J.N. Noordermeer, and L.G. Fradkin. 2008. Src family kinases are required for WNT5 signaling through the Derailed/RYK receptor in the Drosophila embryonic central nervous system. *Development*. 135:2277–2287. doi:10.1242/dev.017319

Yamamoto, H., H. Komekado, and A. Kikuchi. 2006. Caveolin is necessary for Wnt-3a-dependent internalization of LRP6 and accumulation of beta-catenin. *Dev. Cell*. 11:213–223. doi:10.1016/j.devcel.2006.07.003

Yamamoto, H., H. Sakane, H. Yamamoto, T. Michiue, and A. Kikuchi. 2008. Wnt3a and Dkk1 regulate distinct internalization pathways of LRP6 to tune the activation of beta-catenin signaling. *Dev. Cell*. 15:37–48. doi:10.1016/j.devcel.2008.04.015

Yoo, K.-W., E.-H. Kim, S.-H. Jung, M. Rhee, B.-K. Koo, K.-J. Yoon, Y.-Y. Kong, and C.-H. Kim. 2006. Snx5, as a Mind bomb-binding protein, is expressed in hematopoietic and endothelial precursor cells in zebrafish. *FEBS Lett.* 580:4409–4416. doi:10.1016/j.febslet.2006.07.009

Zeng, X., K. Tamai, B. Doble, S. Li, H. Huang, R. Habas, H. Okamura, J. Woodgett, and X. He. 2005. A dual-kinase mechanism for Wnt co-receptor phosphorylation and activation. *Nature*. 438:873–877. doi:10.1038/nature04185

Zhang, C., Q. Li, and Y.-J. Jiang. 2007. Zebrafish Mib and Mib2 are mutual E3 ubiquitin ligases with common and specific delta substrates. *J. Mol. Biol.* 366:1115–1128. doi:10.1016/j.jmb.2006.11.096

Zhong, W., and P.W. Sternberg. 2006. Genome-wide prediction of *C. elegans* genetic interactions. *Science*. 311:1481–1484. doi:10.1126/science.1123287